Using h from Eq. (27), the energy in shear becomes

$$\frac{\Delta w^2}{2} = \frac{u_0^2}{8M^2}\frac{(r/Mr_0)^2}{[1 - 1/2(r/Mr_0)^2]^2} \tag{B2}$$

On the other hand, the energy associated with the adiabatic restoring force of Eq. (6) is

$$\Delta w/w = \Delta T/T = \gamma - 1 \tag{B3}$$

where w is the internal energy, and Δw is the change in w for e-fold expansion. However, from the injection conditions,

$$w = u_0^2/2$$

so that

$$\frac{(\Delta u)^2/2}{w} = \frac{(r/Mr_0)^2}{4M^2(\gamma - 1)[1 - 1/2(r/Mr_0)^2]^2} \tag{B4}$$

For $M^2 = 3$,

$$\frac{(\Delta u)^2/2}{w} = 0.11$$

so that the energy available in velocity shear is small compared to the adiabatic work of perturbation. As a consequence, turbulence should be suppressed everywhere. Equation (B4) is essentially the Richardson[2] number and predicts turbulence close to the value unity.

References

[1] Greenspan, H. P. and Howard, L. N., "On the time-dependent motion of a rotating fluid," J. Fluid Mech. **17**, 385–404 (1963).

[2] Richardson, L. F., "The supply of energy from and to atmospheric eddys," Proc. Roy. Soc. (London) **A97**, 354 (1920).

DECEMBER 1964 AIAA JOURNAL VOL. 2, NO. 12

Stability of Circumferentially Corrugated Sandwich Cylinders under Combined Loads

EDWARD H. BAKER*
North American Aviation, Inc., Downey, Calif.

Theoretical buckling coefficients are obtained for the general instability of simply-supported, corrugated-core, circular sandwich cylinders under combined loads with the corrugations oriented in the circumferential direction. The differential equations of equilibrium which are used to obtain the buckling equations are derived from the small deflection equations of Stein and Mayers which include the effect of deformation due to transverse shear. Approximate solutions to the differential equations are obtained by Galerkin's method. The resulting Galerkin equations are solved for the critical buckling coefficients with the aid of a digital computer. Curves that predict the critical buckling load are presented for axial compression, external lateral pressure, and torsion. In addition, curves are given for the combined loads of axial compression and external lateral pressure, torsion and internal or external lateral pressure, and axial compression and torsion.

Nomenclature

a, b, c, d = Fourier coefficients
A_c = cross-sectional area of core in the xz plane per inch of width, in.
A = $2t$, cross-sectional area of the facing sheets per inch of width, in.
D_c = E_cI_c, flexural rigidity per inch of width of the core in the direction of the corrugations, in.-lb
D = $Eth^2/2(1 - \mu^2)$, flexural stiffness per inch of width of equal thickness isotropic facing sheets about the centroidal axis of the sandwich, in.-lb
D_x, D_y = beam flexural stiffnesses per inch of width of orthotropic plate in axial and circumferential directions, respectively, in.-lb
D_{xy} = twisting stiffness per inch of width and inch of length of orthotropic plate in xy plane, in.-lb
E_c = Young's modulus of elasticity for core material, psi
E = Young's modulus of elasticity for facing material, psi
E_x, E_y = extensional stiffnesses of orthotropic plate in axial and circumferential directions, respectively, lb/in.
G_c = core shear modulus in plane perpendicular to corrugations, psi
G_{xy} = shear stiffness of orthotropic sandwich in xy plane, lb/in.
h = distance between middle surfaces of facing sheets, in.
I_c = moment of inertia per inch of width of the corrugations about the neutral axis of the sandwich composite, in.[3]
J = UL^2/π^2D sandwich cylinder stiffness parameter
K = buckling coefficient
L = length of cylinder, in.
m, s = integers, number of half-waves in the axial direction
n = integer, number of half-waves in the circumferential direction
N_c = force in the axial direction per inch of width acting on the middle plane of the sandwich, lb/in.
N_p = force in the circumferential direction per inch of width acting on the middle plane of the sandwich, lb/in.
N_s = shear force per inch of width acting in the middle plane of the sandwich, lb/in.
p = pressure acting on the cylinder in a directional normal to the plane of the sandwich, psi
Q_x = intensity of transverse force per inch of width acting on cross sections parallel to yz plane, lb/in.
r = radius of cylinder, in.

Received September 27, 1963; revision received July 31, 1964. Part of this paper is based on research completed at the University of California at Los Angeles in partial satisfaction of the requirements for the degree of Master of Science. The author is indebted to S. E. Cain for preparation of the IBM digital computer programs.

* Senior Research Engineer, Applied Mechanics Group, Space and Information Systems Division. Member AIAA.

t	=	thickness of each facing sheet of the sandwich, in.
t_c	=	core depth, in.
t_0	=	thickness of the corrugated core sheet, in.
U	=	$G_c t_c$, elastic core shear stiffness per inch of width in plane perpendicular to corrugations, lb/in.
w	=	total displacement in z direction
x, y, z	=	Cartesian coordinates
Z	=	$L^2/rh(1-\mu^2)^{1/2}$
β	=	$L/2\pi r$, cylinder aspect ratio
μ_x, μ_y	=	Poisson's ratios associated with bending in x and y directions, respectively
μ_x', μ_y'	=	Poisson's ratios associated with extension in x and y directions, respectively
μ	=	Poisson's ratio for the facing sheet material
μ_c	=	Poisson's ratio for the core material

Introduction

THE solution for the general instability of corrugated-core circular sandwich cylinders with the core oriented in the circumferential direction is performed in a manner similar to the solution by Batdorf[1, 2] for the general instability of homogeneous isotropic thin-walled cylinders. In the solution presented and in Batdorf's solution, a differential equation obtained from small deflection theory is solved by Galerkin's[3] method. Batdorf's solution of Donnell's[4] differential equation for homogeneous isotropic circular cylinders is not valid for corrugated sandwich plate because of the low shear stiffness of the sandwich in the plane perpendicular to the corrugations. In the present report, the differential equations are obtained from the small-deflection theory for curved orthotropic sandwich plates by Stein and Mayers.[5] The elastic constants for corrugated-core sandwich were derived from the basic corrugated sandwich geometry and material properties by Libove and Hubka.[6] Stein and Mayers[7] solved for the general instability of sandwich cylinders with longitudinally corrugated core loaded under axial compression in a similar manner. Reference 8 solved for the general instability of longitudinally corrugated core sandwich cylinders loaded under combined loads. The present report takes into consideration axial compression, lateral internal and external pressure, and torsion on circumferentially corrugated cylinders.

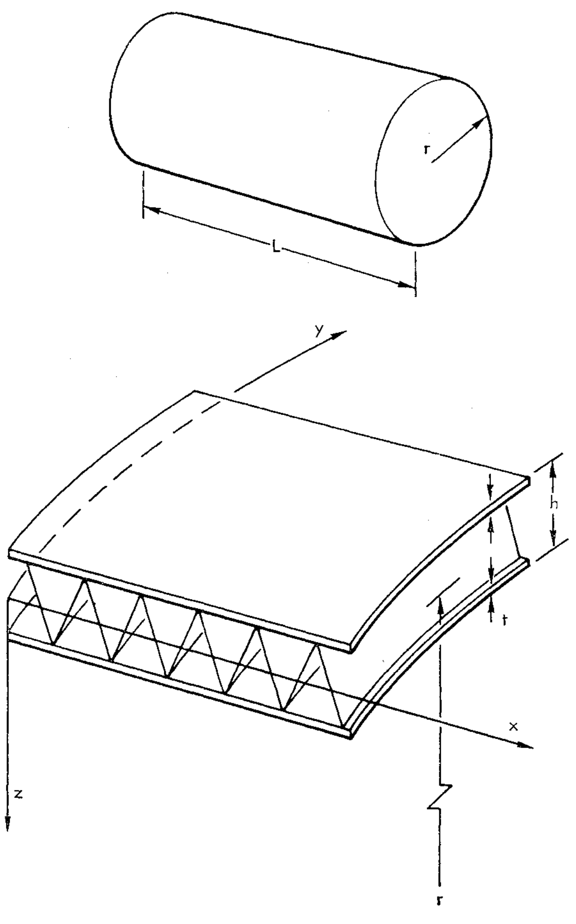

Fig. 1 Circumferentially corrugated sandwich cylinder.

The basic element of the idealized corrugated-core sandwich and the coordinate system are shown in Fig. 1. The element consists of relatively thin isotropic facings that have negligible flexural rigidities about their own centroidal axes and a highly orthotropic core, for which shear distortions are assumed to be admissible only in the x, z plane. Furthermore, the bending rigidity of the core is assumed to be negligible in the x direction. The facings are of equal thickness and are made of the same material. Both the facings and the core are assumed to be elastic. The length and radius of the cylinder are assumed to be large compared with the over-all thickness of the sandwich.

In general, for a corrugated core sandwich, the core shear modulus is many times greater in the plane along the corrugations than it is perpendicular to the corrugations, and the preceding assumption regarding the shear distortion appears to be realistic for many such configurations.

Derivation of Buckling Equations

Figure 1 shows the nomenclature for the sandwich cylinder. The shear stiffness in the yz plane is assumed to be infinite; therefore, the governing differential equations are given by Eqs. (7) and (14) of Ref. 5. The in-plane unit forces in the axial and circumferential directions (N_c and N_p, respectively) are defined as positive in tension in Ref. 5. If N_c and N_p are defined as positive in compression, the differential equations from Ref. 5 may be written as

$$L_D w + \frac{G_{xy}}{r^2} L_E^{-1}\frac{\partial^4 w}{\partial x^4} + \left(N_c\frac{\partial^2 w}{\partial x^2} + N_p\frac{\partial^2 w}{\partial y^2} + 2N_s\frac{\partial^2 w}{\partial x \partial y}\right) - \frac{1}{U}\left[\frac{D_x}{1-\mu_x\mu_y}\frac{\partial^3 Q_x}{\partial x^3} + \left(\frac{\mu_x D_y}{1-\mu_x\mu_y} + D_{xy}\right)\frac{\partial^3 Q_x}{\partial x \partial y^2}\right] = 0 \quad (1)$$

$$Q_x + \frac{D_x}{1-\mu_x\mu_y}\left(\frac{\partial^3 w}{\partial x^3} - \frac{1}{U}\frac{\partial^2 Q_x}{\partial x^2} + \mu_y\frac{\partial^3 w}{\partial x \partial y^2}\right) + \frac{1}{2}D_{xy}\left(2\frac{\partial^3 w}{\partial x \partial y^2} - \frac{1}{U}\frac{\partial^2 Q_x}{\partial y^2}\right) = 0 \quad (2)$$

where

$$L_D = \frac{D_x}{1-\mu_x\mu_y}\frac{\partial^4}{\partial x^4} + \left(\frac{\mu_y D_x}{1-\mu_x\mu_y} + 2D_{xy} + \frac{\mu_x D_y}{1-\mu_x\mu_y}\right)\frac{\partial^4}{\partial x^2 \partial y^2} + \frac{D_y}{1-\mu_x\mu_y}\frac{\partial^4}{\partial y^4}$$

$$L_E = \frac{G_{xy}}{E_y}\frac{\partial^4}{\partial x^4} + \left(1 - \mu_x'\frac{G_{xy}}{E_x} - \mu_y'\frac{G_{xy}}{E_y}\right)\frac{\partial^4}{\partial x^2 \partial y^2} + \frac{G_{xy}}{E_x}\frac{\partial^4}{\partial y^4}$$

$$L_E^{-1}[L_E(w)] = L_E[L_E^{-1}(w)] = w$$

For simply supported edges, the boundary conditions are

$$w = 0 \qquad \frac{\partial^2 w}{\partial x^2} - \frac{1}{D_{Q_x}}\frac{\partial Q_x}{\partial x} + \mu_y\frac{\partial^2 w}{\partial y^2} = 0 \quad \text{at} \quad x = 0, L$$

These conditions are satisfied by the assumed orthogonal deflection function

$$w = \sin\frac{ny}{2r}\sum_{s=1}^{\infty} a_s \sin\frac{s\pi x}{L} + \cos\frac{ny}{2r}\sum_{s=1}^{\infty} b_s \sin\frac{s\pi x}{L} \quad (3)$$

$$Q_x = \sin\frac{ny}{2r}\sum_{s=1}^{\infty} c_s \cos\frac{s\pi x}{L} + \cos\frac{ny}{2r}\sum_{s=1}^{\infty} d_s \cos\frac{s\pi x}{L} \quad (4)$$

where n is restricted to even positive integers equal to or greater than 4, and s is restricted to positive integers equal to or greater than 1.

The solution to Eqs. (1) and (2) is obtained by use of Galerkin's method as described in Ref. 3. The Galerkin equations are

$$\int_0^{2\pi r}\int_0^L R_1(Q_x, w)V_1dxdy = 0 \tag{5a}$$

$$\int_0^{2\pi r}\int_0^L R_1(Q_x, w)V_2dxdy = 0 \tag{5b}$$

$$\int_0^{2\pi r}\int_0^L R_2(Q_x, w)V_3dxdy = 0 \tag{5c}$$

$$\int_0^{2\pi r}\int_0^L R_2(Q_x, w)V_4dxdy = 0 \tag{5d}$$

where

$$V_1 = \sin\frac{ny}{2r}\sin\frac{m\pi x}{L} \qquad V_2 = \cos\frac{ny}{2r}\sin\frac{m\pi x}{L}$$

$$V_3 = \cos\frac{ny}{2r}\cos\frac{m\pi x}{L} \qquad V_4 = \sin\frac{ny}{2r}\cos\frac{m\pi x}{L}$$

The expression for $R_1(Q_x, w)$ is obtained by substituting Eqs. (3) and (4) into Eq. (1) and that for $R_2(Q_x, w)$ is obtained by substituting Eqs. (3) and (4) into Eq. (2).

$$\beta = \frac{L}{2\pi r} \qquad Z = \frac{L^2}{rh}(1-\mu^2)^{1/2} \qquad J = \frac{UL^2}{\pi^2 D}$$

$$D = \frac{Eth^2}{2(1-\mu^2)} \qquad D_c = E_cI_c \qquad \delta_1 = \frac{1}{1+(E_cA_c/EA)}$$

$$\delta_2 = \frac{1+\mu}{1+[(1+\mu)/(1+\mu_c)](t_0/A_c)^2E_cA_c/EA} - \mu\frac{EA}{EA+E_cA_c}$$

$$\delta_3 = 1 - \mu^2\frac{1}{1+(EA/E_cA_c)} \qquad K_p = \frac{N_pL^2}{\pi^2D} = \frac{prL^2}{\pi^2D}$$

$$K_c = \frac{N_cL^2}{\pi^2D} \qquad K_s = \frac{N_sL^2}{\pi^2D}$$

With the introduction of these parameters, Eqs. (6) and (7) are simplified to the following form:

$$Aa_m - K_s\frac{8\beta n}{\pi m^2}\sum_{s=1}^{\infty} b_s\frac{ms}{m^2-s^2} = 0 \tag{8}$$

$$Ab_m + K_s\frac{8\beta n}{\pi m^2}\sum_{s=1}^{\infty} a_s\frac{ms}{m^2-s^2} = 0 \tag{9}$$

After the proper substitution and integration have been performed on Eqs. (5a) and (5d), Eq. (5d) is solved for c_m, which is substituted in Eq. (5a). The following equation results:

$$\left\{\frac{D_x}{1-\mu_x\mu_y}\frac{\pi^4m^4}{L^4} + \left(\frac{\mu_yD_x}{1-\mu_x\mu_y} + 2D_{xy} + \frac{\mu_xD_y}{1-\mu_x\mu_y}\right)\left(\frac{n}{2r}\right)^2\left(\frac{\pi m}{L}\right)^2 + \frac{D_y}{1-\mu_x\mu_y}\left(\frac{n}{2r}\right)^4 + \frac{\dfrac{G_{xy}}{r^2}\left(\dfrac{\pi m}{L}\right)^4}{\dfrac{G_{xy}}{E_y}\dfrac{\pi^4m^4}{L^4} + \left(1-\mu_x'\dfrac{G_{xy}}{E_x} - \mu_y'\dfrac{G_{xy}}{E_y}\right)\dfrac{n^2\pi^2m^2}{4r^2L^2} + \dfrac{G_{xy}}{E_x}\left(\dfrac{n}{2r}\right)^4} - \left[\frac{D_x}{U(1-\mu_x\mu_y)}\left(\frac{\pi m}{L}\right)^3 + \frac{1}{U}\left(\frac{n}{2r}\right)^2\frac{\pi m}{L}\left(\frac{\mu_xD_y}{1-\mu_x\mu_y} + D_{xy}\right)\right]\times \left[\frac{\dfrac{(\pi m/L)^3D_x}{1-\mu_x\mu_y} + \dfrac{D_x\mu_y}{1-\mu_x\mu_y}\left(\dfrac{n}{2r}\right)^2\dfrac{\pi m}{L} + D_{xy}\left(\dfrac{n}{2r}\right)^2\dfrac{\pi m}{L}}{1 + \dfrac{D_x(\pi m/L)^2}{(1-\mu_x\mu_y)U} + \dfrac{D_{xy}}{2U}\left(\dfrac{n}{2r}\right)^2}\right] - N_c\left(\frac{\pi m}{L}\right)^2 - N_p\left(\frac{n}{2r}\right)^2\right\}a_m - N_s\frac{4n}{rL}\sum_{s=1}^{\infty}\frac{ms}{m^2-s^2}b_s = 0 \tag{6}$$

where $m \pm s$ = odd integers.

In a similar manner, after the proper substitution and integration have been performed on Eqs. (5b) and (5c), Eq. (5c) is solved for d_m, which is substituted into Eq. (5b). The following equation results after substitution and simplification:

$$\left\{\frac{D_x}{1-\mu_x\mu_y}\frac{\pi^4m^4}{L^4} + \left(\frac{\mu_yD_x}{1-\mu_x\mu_y} + 2D_{xy} + \frac{\mu_xD_y}{1-\mu_x\mu_y}\right)\left(\frac{n}{2r}\right)^2\left(\frac{\pi m}{L}\right)^2 + \frac{D_y}{1-\mu_x\mu_y}\left(\frac{n}{2r}\right)^4 + \frac{\dfrac{G_{xy}}{r^2}\left(\dfrac{\pi m}{L}\right)^4}{\dfrac{G_{xy}}{E_y}\dfrac{\pi^4m^4}{L^4} + \left(1-\mu_x'\dfrac{G_{xy}}{E_x} - \mu_y'\dfrac{G_{xy}}{E_y}\right)\dfrac{n^2\pi^2m^2}{4r^2L^2} + \dfrac{G_{xy}}{E_x}\left(\dfrac{n}{2r}\right)^4} - \left[\frac{D_x}{U(1-\mu_x\mu_y)}\left(\frac{\pi m}{L}\right)^3 + \frac{1}{U}\left(\frac{n}{2r}\right)^2\frac{\pi m}{L}\left(\frac{\mu_xD_y}{1-\mu_x\mu_y} + D_{xy}\right)\right]\times \left[\frac{\dfrac{(\pi m/L)^3D_x}{1-\mu_x\mu_y} + \dfrac{D_x\mu_y}{1-\mu_x\mu_y}\left(\dfrac{n}{2r}\right)^2\dfrac{\pi m}{L} + D_{xy}\left(\dfrac{n}{2r}\right)^2\dfrac{\pi m}{L}}{1 + \dfrac{D_x(\pi m/L)^2}{(1-\mu_x\mu_y)U} + \dfrac{D_{xy}}{2U}\left(\dfrac{n}{2r}\right)^2}\right] - N_c\left(\frac{\pi m}{L}\right)^2 - N_p\left(\frac{n}{2r}\right)^2\right\}b_m + N_s\frac{4n}{rL}\sum_{s=1}^{\infty}\frac{ms}{m^2-s^2}a_s = 0 \tag{7}$$

where $m \pm s$ = odd integers.

Formulas for the physical constants μ_x, μ_y, μ_x', μ_y', D_x, D_y, D_{xy}, E_x, E_y, and G_{xy} are obtained from Ref. 6 and substituted into Eqs. (6) and (7). The resulting equations may be simplified by introducing the following geometric and material parameters:

where $m \pm s$ = odd integers and

$$A = \frac{D_c}{D}\frac{n^4\beta^4}{m^2} + \frac{[m^2+n^2\beta^2]^2[2J+n^2\beta^2(1-\mu)]}{[2J+n^2\beta^2(1-\mu)+2m^2]m^2} + \frac{4Z^2m^2}{\pi^4[\delta_1m^4+2\delta_2n^2\beta^2m^2+\delta_3\beta^4n^4]} - K_c - K_p\frac{\beta^2n^2}{m^2}$$

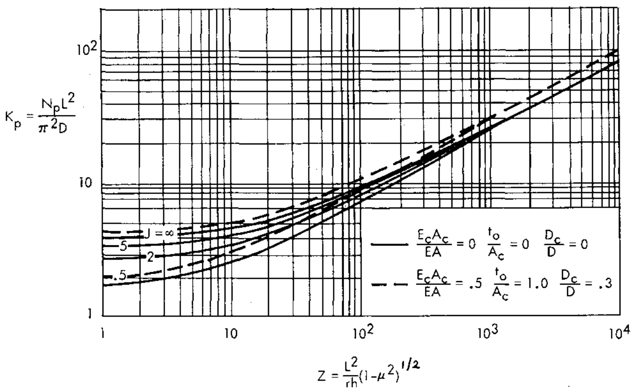

Fig. 2 Buckling coefficients for external lateral pressure.

The critical buckling coefficients K_p, K_c, and K_s can be obtained from Eqs. (8) and (9) for a given set of geometric and material parameters.

Mathematical Solutions for Buckling Coefficients

The buckling coefficients for circumferentially corrugated circular sandwich cylinders may be obtained from Eqs. (8) and (9) for given sets of parameters. In these solutions, m is restricted to positive integers and n is restricted to even positive integers equal to or greater than 4.

Solution for K_p; K_c and $K_s = 0$

Any of the equations represented in Eqs. (8) and (9) may be used to solve for K_p, if K_s is equal to zero, because the equations are independent for this case.

If K_c and K_s are 0, close inspection of the equation reveals that, if m is restricted to positive integers, K_p will be a minimum for $m = 1$ and the equation can be written in the form

$$K_p = \frac{n^2\beta^2 D_c}{D} + \frac{[1 + n^2\beta^2]^2[2J + n^2\beta^2(1-\mu)]}{[2J + n^2\beta^2(1-\mu) + 2]n^2\beta^2} + \frac{4Z^2}{\pi^4[\delta_1 + 2\delta_2 n^2\beta^2 + \delta_3\beta^4 n^4]n^2\beta^2} \qquad (10)$$

A digital computer program was coded to solve Eq. (10) for various values of n until the minimum value of K_p was found for the chosen parameters. A plot of K_p as a function of Z is shown in Fig. 2 for various values of J.

Solution for K_c; K_p Known: $K_s = 0$

Any of the equations represented by Eqs. (8) and (9) may be used to solve for K_c if K_s is equal to zero, because each of the equations is independent. If K_s is equal to zero, Eq. (8) or (9) may be written in the form

$$K_c = \frac{D_c}{D}\frac{n^4\beta^4}{m^2} + \frac{[m^2 + n^2\beta^2]^2[2J + n^2\beta^2(1-\mu)]}{[2J + n^2\beta^2(1-\mu) + 2m^2]m^2} + \frac{4Z^2m^2}{\pi^4[\delta_1 m^4 + 2\delta_2 n^2\beta^2 m^2 + \delta_3\beta^4 n^4]} - K_p\beta^2\frac{n^2}{m^2} \qquad (11)$$

A digital computer program was coded to solve Eq. (11) for various combinations of m and n until the minimum value of K_c was found for the chosen geometric and material parameters and for a specified value of K_p. Figure 3 is a plot of K_c as a function of Z for the special case of $K_p = 0$. Figures 4 and 5 are plots of K_c as a function of K_p for values of Z of 10 and 10^3.

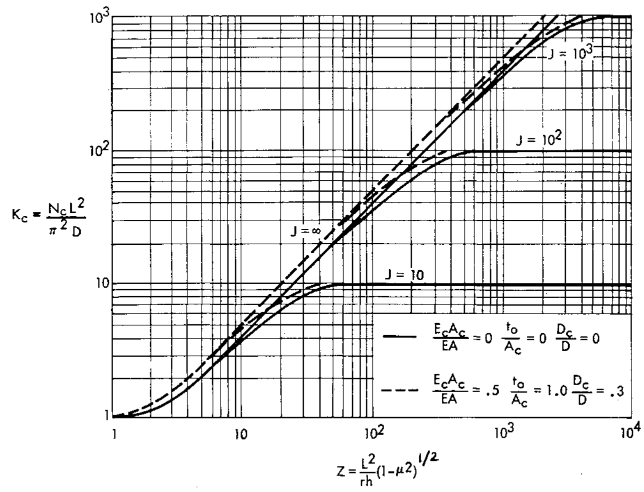

Fig. 3 Buckling coefficients for axial compression.

Solution for K_s; K_p and K_c Known

Each of the equations represented by Eq. (8) may be expressed in the form

$$Aa_m - \lambda^{-1}Bb_s = 0 \qquad (12)$$

Each of the equations represented by Eq. (9) may be expressed in the form

$$Ab_m + \lambda^{-1}Ba_s = 0 \qquad (13)$$

where $m \pm s =$ odd integers, and

$$B = \frac{8\beta n}{\pi m^2}\sum_s \frac{sm}{m^2 - s^2} \qquad \lambda^{-1} = K_s$$

In matrix form, these equations become

$$\lambda\{a\} = [G_1]\{b\} \qquad (14)$$

$$\lambda\{b\} = -[G_1]\{a\} \qquad (15)$$

where λ is a scalar, and

$$[G_1] = [A]^{-1}[B]$$

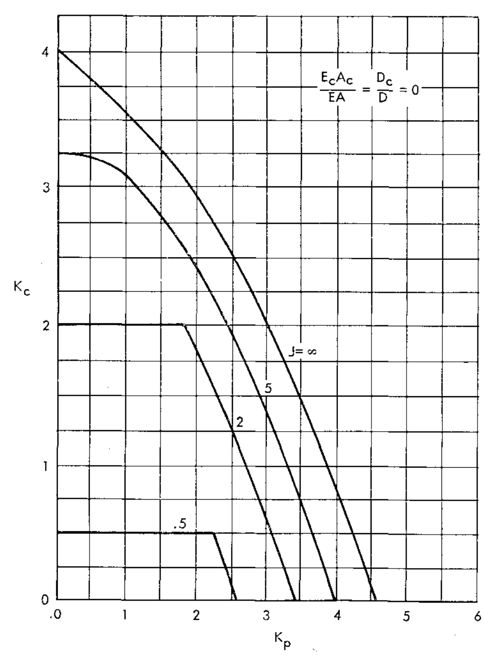

Fig. 4 Buckling coefficients for combined lateral pressure and axial compression for $Z = 10^3$.

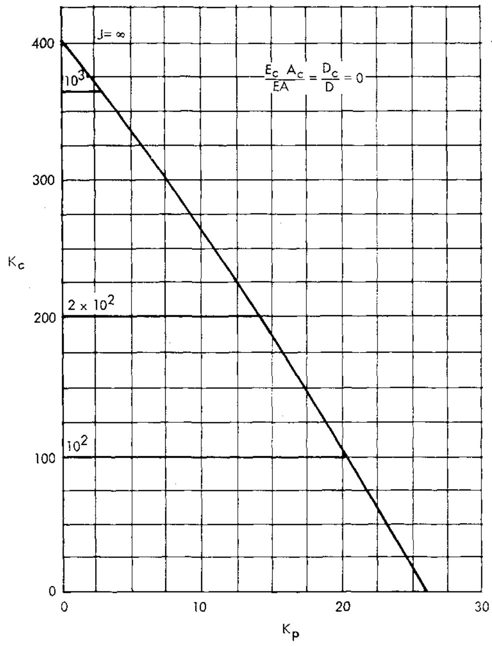

Fig. 5 Buckling coefficients for combined lateral pressure and axial compression for $Z = 10^3$.

The solution for λ by matrix iteration is complicated by the fact that the cylinder will buckle at a load level that is independent of the direction of the applied shear. Therefore, the buckling coefficients and corresponding eigenvalues occur in pairs that are equal in magnitude but opposite in sign. Solving Eq. (15) for the column matrix on the left-hand side and substituting into Eq. (14) results in the following equations:

$$\lambda^2\{a\} = [G_2]\{a\}$$

where

$$[G_2] = [G_1][-G_1]$$

The matrix G_2 can be formed either from Eq. (12) or (13). An 8×8 matrix was formed and iterated using a computer program to obtain the eigenvalue λ^2. The iteration continued until the scalar λ^2 remained constant to six significant figures. The buckling coefficient K_s is the square root reciprocal of the eigenvalue λ^2:

$$K_s = (1/\lambda^2)^{1/2}$$

The matrix G_1, used to form the 8×8 G_2 matrix, was of the following form:

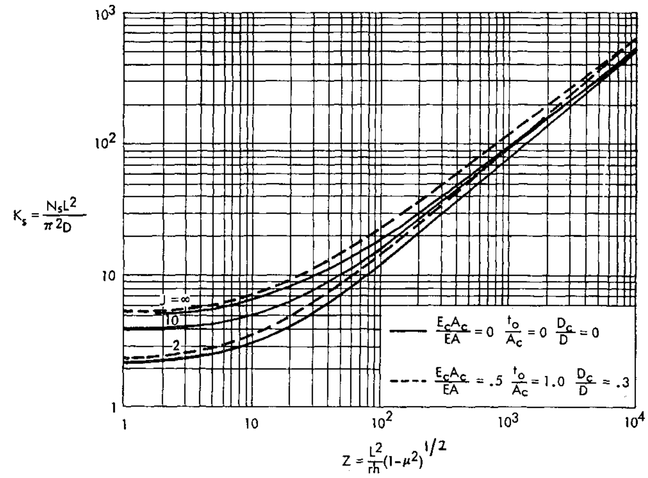

Fig. 6 Buckling coefficients for torsion.

where A_i is the value of A for $m = i, i = 1, 8$, and

$$B_{ms} = (8\beta n/\pi m^2)sm/(m^2 - s^2)$$

The parameter n is a constant for a particular G_1 matrix.

By the proper interchanging of rows and columns, the same value of K_s could have been obtained by iterating a 4×4 matrix instead of an 8×8.

For a given set of numerical values of the sandwich parameters, buckling coefficients are obtained for single values of n until the minimum value of the buckling coefficients is found. Figure 6 is a plot of K_s as a function of Z for the special case of K_c and K_p equal to 0. Figures 7 and 8 are plots of K_s as a function K_c for values of Z equal to 10 and 10^3. Figures 9 and 10 are plots of K_p as a function of K_s for values of Z equal to 10 and 10^3.

Comparison with Other Solutions

Cylinders

The method of solution used for the corrugated sandwich cylinders is the same as that used for homogeneous isotropic cylinders in Refs. 1 and 2. Therefore, if the parameters for a sandwich, which is the equivalent of a homogeneous sheet, are substituted into the sandwich cylinder stability equations, the resulting equations should be the same as the equations presented in Refs. 1 and 2.

A sandwich with $U = \infty$, $D_c/D = 0$, $E_cA_c/EA = 0$, and $t = h$ is the equivalent of homogeneous sheet. For the case

$$[G_1] = \begin{array}{c} \\ m=1 \\ m=2 \\ m=3 \\ m=4 \\ m=5 \\ m=6 \\ m=7 \\ m=8 \end{array}
\begin{array}{c} \begin{array}{cccccccc} s=1 & s=2 & s=3 & s=4 & s=5 & s=6 & s=7 & s=8 \end{array} \\
\left[\begin{array}{cccccccc}
0 & \frac{B_{12}}{A_1} & 0 & \frac{B_{14}}{A_1} & 0 & \frac{B_{16}}{A_1} & 0 & \frac{B_{18}}{A_1} \\
\frac{B_{21}}{A_2} & 0 & \frac{B_{23}}{A_2} & 0 & \frac{B_{25}}{A_2} & 0 & \frac{B_{27}}{A_2} & 0 \\
0 & \frac{B_{32}}{A_3} & & & & & & \\
\frac{B_{41}}{A_4} & 0 & & & & & & \\
0 & \frac{B_{52}}{A_5} & & & \text{etc.} & & & \\
\frac{B_{61}}{A_6} & 0 & & & & & & \\
0 & \frac{B_{72}}{A_7} & & & & & & \\
\frac{B_{81}}{A_8} & 0 & & & & & &
\end{array}\right] \end{array}$$

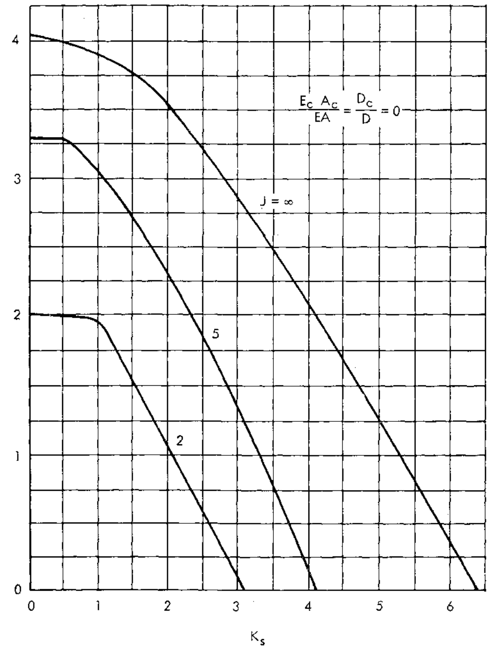

Fig. 7 Buckling coefficients for combined axial compression and torsion for $Z = 10$.

of $t = h$, the moment of inertia of the facing sheets about their own centroid cannot be neglected so that I is equal to $2/3\ t^3$. With this correction, the equation becomes

$$\left[\frac{(m^2 + \beta_0{}^2)^2}{m^2} + \frac{12Z_0m^2}{\pi^4(m^2 + \beta_0{}^2)^2} - K_c - K_p\frac{\beta_0{}^2}{m^2}\right]a_m - K_s\frac{8\beta_0}{\pi m^2}\sum_s b_s\frac{ms}{m^2 - s^2} = 0 \quad (16)$$

where

$$\beta_0 = nL/2\pi r,\ Z_0 = (L^2/rt_H)(1 - \mu^2)^{1/2},\ t_H = 2t$$

This equation is the same as the equations given in Refs. 1 and 2 for cylinders of homogeneous isotropic sheet.

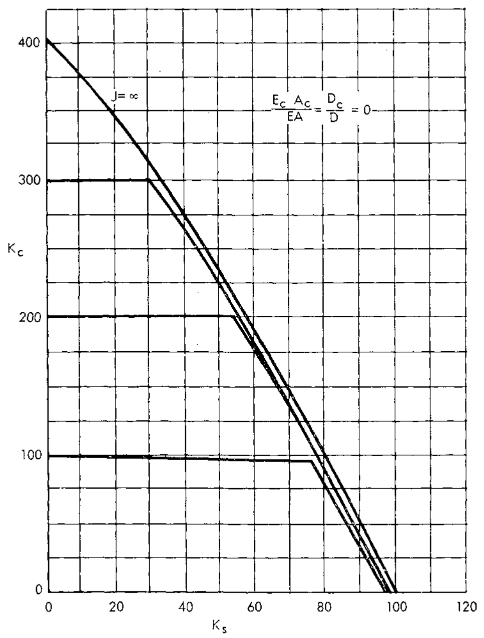

Fig. 8 Buckling coefficients for combined axial compression and torsion for $Z = 10^3$.

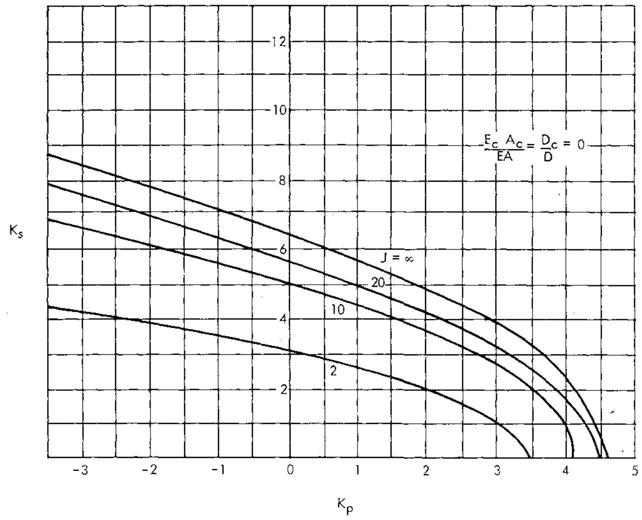

Fig. 9 Buckling coefficients for combined lateral pressure and torsion for $Z = 10$.

Comparison with Results for Flat Plates

As the value of Z for a cylinder becomes very small, the radius of the cylinder becomes very large, and the cylinder behaves like an infinitely wide plate. Therefore, at very low values of Z, the buckling coefficients of cylinders should be the same as the buckling coefficients either for a geometrically similar infinitely wide or infinitely long flat plate that is loaded in the same manner with the core oriented properly.

The buckling coefficients for the pure load case of shear at $Z = 1$ were compared with the appropriate buckling coefficients given in Ref. 9 for flat corrugated sandwich plates with aspect ratios of approximately 3. The buckling coefficients for the flat plates were a maximum of 15% higher than the buckling coefficients for cylinders with $Z = 1$, with most variations 5% or less. The buckling coefficients probably would be much closer if the length-to-width ratio of the plate were larger.

For the case of axial compression of a cylinder with a very large radius, Eq. (11) becomes

$$K_c = m^2/[1 + (m^2/J)]$$

K_c is a minimum for $m = 1$,

$$K_c = 1/[1 + (1/J)] \quad (17)$$

The buckling of a column with shear deformations included is presented in Ref. 10. It is valid for an infinitely wide

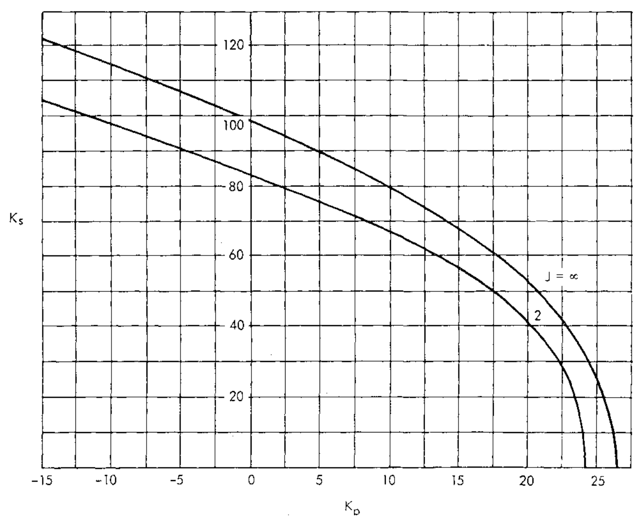

Fig. 10 Buckling coefficients for combined lateral pressure and torsion for $Z = 10^3$.

Table 1 Effect of L/r on K_p; $J = \infty$, $D_c/D = 0$, $E_cA_c/EA = 0$

L/r	Z	1	5	10	5×10	10^2	5×10^2	10^3	5×10^3	10^4	5×10^4	10^5
0.1	n	64	68	76	120	146	...	...	...	...	...	...
	K_p	4.011	4.211	4.606	7.225	9.440	...	...	...	...	...	...
0.5	n	12	14	16	24	30	44	54	80	96	...	...
	K_p	4.021	4.211	4.606	7.225	9.478	19.11	26.39	57.25	80.35	...	...
1.0	n	6	6	8	12	14	22	26	40	48	72	86
	K_p	4.021	4.318	4.606	7.225	9.494	19.11	26.49	57.25	80.35	178.0	251.1
10.0	n	...	...	...	...	...	...	...	4	6	8	8
	K_p	...	...	...	...	...	...	...	57.25	98.35	187.7	259.6

plate if the moment of inertia of the column is replaced by the flexural rigidity of the plate. The critical buckling load presented in Ref. 10 would then agree with Eq. (17) if Dc/D were small in comparison to unity.

Upper Bound Axial Compression

If the value of m is set equal to infinity in Eq. (14) and $K_p = 0$, the resulting expression is

$$K_c = J + (n^2\beta^2/2)(1 - \mu)$$

If the loading case is axial compression and $(mr/L)^2$ is very large in comparison to l, the theory that has been presented is valid for small values of n. The value of K_c is a minimum for the expression given previously if $n = 0$. Therefore, $K_c = J$ or $N_c = U = G_ct_c$.

This places an upper bound on the buckling coefficient of a circumferentially corrugated sandwich cylinder which is subjected to axial compression. This can be seen in Fig. 3. The buckling curve for a finite value of J increases with increased Z until it approaches a value of K_c which is equal to the value of J. At this point the curve becomes asymptotic to the value $K_c = J$.

When the critical load per inch equals the shear rigidity, the mode of failure is called crimping because the wavelength of the buckle is extremely short. This upper bound has been derived in all stability investigations that analyze sandwich plates and shells subjected to compressive forces in the direction of the sandwich that has finite shear rigidity. This upper bound can be seen in the stability curves for flat sandwich plates with either isotropic or corrugated core as well as the stability curves for sandwich cylinders with isotropic core. In addition, this upper bound was arrived at in a large deflection theory of sandwich cylinders subjected to axial compression.[11] Therefore, it is believed that curves presented for axial compression of circumferentially corrugated sandwich cylinders subjected to axial compression are valid in the range of $K_c = J$.

Effect of Geometric and Material Parameters

Stiffness Ratios

The parameters E_cA_c/EA, t_0/A_c, and D_c/D were investigated to determine their effect on the buckling coefficients. It can be seen from Eqs. (10) and (11) that, if any of these three parameters are increased while the remaining parameters are kept constant, the buckling coefficient is also increased. However, the effect on the critical buckling coefficient of varying E_cA_c/EA, t_0/A_c, and D_c/D through their practical range is small. This insensitivity to changes in the stiffness ratios is indicated in Figs. 2, 3, and 6 in which the solid curves are the buckling coefficients for cylinders with $E_cA_c/EA = 0$, $t_0/A_c = 0$, and $D_c/D = 0$, and the dashed lines are the buckling curves for $E_cA_c/EA = 0.5$, $t_0/A_c = 1.0$, and $D_c/D = 0.3$. The latter values of these parameters are believed to be about as high as can be achieved in practical applications, provided the sandwich material remains in the elastic range. It can be seen that the maximum differences between the dashed and solid curves are only about 20%. Therefore, the solid curves can be used as a conservative close approximation to the critical buckling coefficient.

Effect of L/r on the Buckling Coefficients

If the value of L/r is varied in the buckling equation and all of the other parameters are kept constant, the critical buckling coefficient will also vary slightly. This variation is caused mainly by the fact that n is restricted to even integer values. If n could vary freely, the critical buckling coefficients for a given value of Z would be independent of the L/r ratio. If n is restricted to even integer values, cylinders with higher values of L/r often have slightly higher buckling coefficients.

The effect of L/r on the buckling coefficient is shown in Table 1 for the case of external pressure with $J = \infty$. It can be seen that the effect is small except for $L/r = 10$. Because the effect of L/r on the critical buckling coefficient was small, curves were not presented for the various values of L/r. The curves given were obtained with L/r values which resulted in critical values of n large enough so that the buckling coefficients would be very close to the absolute minimum of the equation. Therefore, the curves generally will be on the conservative side.

Conclusion

The theory and curves presented in the previous sections have been compared against existing theoretical results for the case of $Z = 1$ and $J = \infty$ as well as for the case of axial compression with relatively low shear modulus. The comparison at these extremes showed close agreement, and it is believed that the buckling curves presented in this report are valid within the limitations of small-deflection theory. For the cases of cylinders subjected to external pressure and/or torsion, small-deflection theory appears to be an adequate tool for predicting the buckling phenomena. This can be seen from Ref. 1, which derives the buckling curves for monocoque cylinders in a manner similar to method presented herein and compares the results with test data. For the case of external pressure or torsion, the agreement between theory and tests was quite good, and it is believed that test data of circumferentially corrugated sandwich cylinders subjected to external pressure, torsion, or combinations of the two will be in reasonable agreement with the theory that has been presented.

The buckling phenomena of homogeneous isotropic cylinders subjected to axial compression have not been well represented by small-deflection theory. Therefore, the results that have been presented for circumferentially corrugated sandwich cylinders under axial compression may predict buckling loads that are too high. However, for the limiting case in which shear distortion becomes predominant, the large-deflection theory presented in Ref. 10 predicts the same critical load as presented in Fig. 3 ($N_c = G_ct_c$), and the test results in Ref. 10 agree well with the theory for sandwich cylinders with relatively low shear stiffness. The accuracy of small-deflection theory for predicting the critical axial compression buckling load of a sandwich cylinder with relatively high transverse shear rigidity can only be determined by an extensive series of tests.

The orientation of the core is an important design consideration for a corrugated core sandwich cylinder. The direction to orient the core is dependent upon the loading condition. Through the use of Figs. 2–10 and Ref. 8, the most efficient core orientation may be chosen for corrugated core sandwich cylinders.

If U is a set equal to infinity, Eqs. (7) and (8) are the small-deflection buckling equations for an orthotropic cylinder including the effects of Poisson's ratio. Equations (7) and (8) may then be used to determine the general instability under combined loads of a stiffened cylinder with relatively close stiffeners that are orientated in any direction by using the elastic constants presented in Ref. 12.

References

[1] Batdorf, S. B., "A simplified method for elastic stability analysis for thin cylindrical shells," NACA Rept. 874 (1947).

[2] Batdorf, S. B., Stein, M., and Schildcrout, M., "Critical stress of thin walled cylinders in torsion," NACA TN 1344, (June 1947).

[3] Wang, C., *Applied Elasticity* (McGraw-Hill Book Co., Inc., New York, 1953).

[4] Donnell, L. H., "Stability of thin walled tubes under torsion," NACA Rept. 479 (1933).

[5] Stein, M. and Mayers, J., "A small deflection theory for curved sandwich plates," NACA TN 2017 (February 1950).

[6] Libove, C. and Hubka, R., "Elastic constants for corrugated core sandwich plates," NACA TN 2289 (February 1951).

[7] Stein, M. and Mayers, J., "Compressive buckling of simply supported curved plates and cylinders of sandwich construction," NACA TN 2601 (January 1952).

[8] Harris, L. A. and Baker, E. H., "Elastic stability of simply supported corrugated core sandwich cylinders," NASA TN D-1510.

[9] Harris, L. A. and Auelmann, R. R., "Stability of flat simply supported corrugated core sandwich plates under combined loads," J. Aerospace Sci. **27,** 525–34 (July 1960).

[10] Timoshenko, S. and Gere, J., *Theory of Elastic Stability* (McGraw-Hill Book Co., Inc., New York, 1961), 2nd ed.

[11] March, H. W. and Kuenzi, E. W., "Buckling of cylinders of sandwich construction in axial compression," Forest Products Lab. Rept. 1830 (December 1957).

[12] Dow, N., Libove, C., and Hubka, R., "Formulas for the elastic constants of plates with integral waffe-like stiffening," NACA RM L53E13a (August 1953).